PHYSICAL REVIEW E **112**, 015415 (2025)

Thermodynamic potential of ferroelectric nematic liquid crystals and consequences for polarization switching

Diana Nikolova,[1,*] Rachel Tuffin,[2] Helen F. Gleeson,[1] and Mikhail Osipov[3]
[1]*School of Physics and Astronomy, University of Leeds, Leeds LS2 9JT, United Kingdom*
[2]*Merck Electronics KGaA, Frankfurter Strasse 250, 64293 Darmstadt, Germany*
[3]*Department of Mathematics and Statistics, University of Strathclyde, Glasgow G1 1XH, United Kingdom*

(Received 10 March 2025; accepted 13 June 2025; published 17 July 2025)

The ferroelectric nematic (N_f) liquid crystal phase is a highly polar fluid, with spontaneous polarization (P_S) values of the order of μC cm^{-2} and viscosities of around 10 Pas. The combination of high polarity and fluidity makes these materials unique polar dielectrics. We consider the free energy of the ferroelectric nematic phase and derive its thermodynamic potentials. This allows us to predict that the spontaneous polarization will saturate as a function of applied voltage, rather than field. Further, we determine that the inclusion of an alignment layer, which is usual in liquid crystal devices, could provide a significantly enhanced energy barrier to switching. Indeed, an insulating alignment layer introduces a polar anchoring energy in addition to the orientational anchoring energy usually considered in liquid crystal devices. We confirm experimentally that measurements of the spontaneous polarization depend very slightly on the thickness of the N_f layer and more dramatically on the polar interactions of the phase with the confining surfaces. In relatively thin devices (∼10 μm) with an alignment layer present, we demonstrate that this effect can be so pronounced that polarization switching is completely suppressed. We also explore the influence of the preparation conditions of a thin film of ferroelectric nematic material on the stability and lifetime of the sample.

DOI: 10.1103/cdnd-8g98

I. INTRODUCTION

Nearly all ferroelectric materials are solids, whether crystals, ceramics, polymers, or plastic crystals, with liquid crystals (LCs) offering the only known ferroelectric fluid systems [1]. LCs are fluids in which different symmetries and order define both the phase and its bulk properties. The most common LC state is the (apolar) nematic (N) phase which has orientational order only and which has been ubiquitous in display devices since the 1980s. The first known ferroelectric LCs were smectic systems, characterized by chirality together with orientational and one-dimensional positional order (layers) and values of spontaneous polarization (P_S) much smaller than those seen in solid systems (nC cm^{-2} rather than μC cm^{-2} respectively) [2]. The discovery in 2017 of the ferroelectric nematic (N_f) phase, with spontaneous polarization comparable to that seen in solid ferroelectrics [3,4], was heralded as a breakthrough; such materials had been predicted as long ago as 1916 [5] and the potential for new kinds of applications was readily seen. However, what was perhaps less obvious was that these highly macroscopically polar fluids behave subtly differently from both solid ferroelectrics and the far less polar, rather viscous, ferroelectric smectic LCs; one must naturally expect to see them behave in new ways, and moreover to reexamine the techniques used to study them and what assumptions are made.

The ferroelectric nematic (N_f) phase differs from the N phase specifically by breaking the director inversion symmetry $\vec{n} \equiv -\vec{n}$, resulting in local bulk polarity (see Fig. 1). A characteristic of N_f materials is the large molecular dipole moment of the molecules that form the phase; for example, for the first N_f materials discovered, it takes values of $\mu \sim 11$ D for RM734 [6] and ∼10 D for DIO [4]. The body of work characterizing the properties of ferroelectric nematic LCs (FNLCs) is already impressive, probing into the multitude of interesting properties the phase exhibits: instabilities that could be manipulated for optical applications; formation of large polar domains; interesting electrooptic responses; large phototunable dielectric permittivity; and tunable nonlinear optic coefficients, to name a few [7–13].

As an essential property of ferroelectric materials, the spontaneous polarization (P_S), is the focus of this work. It is well known that in conventional ferroelectric crystals the polarization switching is mainly determined by nucleation of new domains or by the movement of domain walls (at higher fields). In some materials one finds a direct reversal of the microscopic dipoles under the action of the electric field. It is also the case that the domain structure in ferroelectric crystals cannot be completely removed by any reasonable electric field used for switching. On the other hand, the polarization switching mechanism in the ferroelectric nematic phase is not completely clear. Indeed, the fluid nature and nematic

---

[*] Contact author: py18dn@leeds.ac.uk

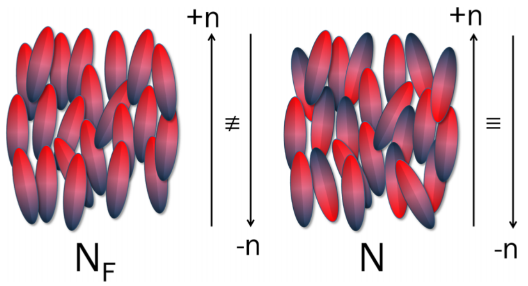

FIG. 1. Illustration showing the difference between the N_f and N phases. The molecules are represented by ellipsoids with the dipole moment indicated by the differently coloured ends.

ordering in N_f materials means that strong polarity will govern their behavior, including during switching; in an apolar nematic LC, one might expect instead to observe behavior influenced by the positional and orientational geometries of the phase. Various domain structures and inhomogeneous polarization profiles, which minimize the total electrostatic energy, can be found in FNLCs with disconnected electrodes. However, in contrast to solid ferroelectrics, these domain structures can be removed by a relatively small applied voltage because the polarization may easily rotate in the bulk and the energy cost of orientational deformations is relatively low. In principle, the spontaneous polarization may even rotate homogeneously if the surface potential barriers are sufficiently small.

In this paper, we consider the free energy of the ferroelectric nematic phase, allowing us to predict and confirm experimentally the consequences for their polarization switching. Specifically, we present a derivation of the thermodynamic potentials for N_f materials in a standard thin cell geometry, noting the contribution due to inhomogeneous polarization in a polar fluid, and posit that the switching behavior under an applied voltage is determined primarily by the presence and size of a potential energy barrier which must be overcome. In that vein, we propose that the polarization response in the N_f phase depends on voltage rather than field, which we demonstrate experimentally. We explore how it is affected also by varying the surface boundary and anchoring conditions, sample preparation conditions, and sample thickness, demonstrating and explaining how the presence of an alignment layer can increase the potential barrier, to the extent where it cannot be overcome in thinner cells. Thus, ferroelectric switching is simply not observed at any reasonable voltage.

II. THEORETICAL DISCUSSION

A. Potential energy barrier and dependence on applied voltage

The dependence of the polarization on the external electric field in a ferroelectric material can be described using the general expression for the free energy. At present there is no consistent derivation of the thermodynamic potentials of FNLCs in the literature, and various models have been used by different authors. In this section we present a general derivation of the two thermodynamic potentials for a flat ferroelectric cell such as those described later in the paper.

One notes that in the general description of ferroelectric materials (both solid crystals and polar nematic LCs) one should consider two conjugated thermodynamic potentials which depend on the electric field $\boldsymbol{E}$ and on the electric induction $\boldsymbol{D}$ (see, for example, the seminal book of Landau and Lifschitz [14,15]). In particular, the thermodynamic potential $F(T,\boldsymbol{E})$ can be used to describe the properties of the ferroelectric material at fixed macroscopic electric fields in the medium $\boldsymbol{E}$, i.e., at fixed applied voltage and at a temperature T. At the same time the potential $G(T,\ \boldsymbol{D})$ describes the ferroelectric material at fixed induction $\boldsymbol{D}$, i.e., at fixed charges at the electrodes. These two conjugate potentials are related by the following Legendre transformation:

$$F(T,\boldsymbol{E}) = G(T,\ \boldsymbol{D}) - \ \boldsymbol{E}\cdot\boldsymbol{D}. \tag{1}$$

Here the electric field at fixed $\boldsymbol{D}$ is expressed as the derivative of the potential $G(T,\ \boldsymbol{D})$:

$$\boldsymbol{E} = \left.\frac{\partial G(T,\boldsymbol{D})}{\partial \boldsymbol{D}}\right|_T \tag{2}$$

while the electric induction $\boldsymbol{D}$ at fixed electric field $\boldsymbol{E}$ is determined by the derivative of $F(T,\boldsymbol{E})$:

$$\boldsymbol{D} = -\left.\frac{\partial F(T,\boldsymbol{E})}{\partial \boldsymbol{E}}\right|_T. \tag{3}$$

The two conjugate potentials can be used to describe any dielectric materials, while the properties of the ferroelectric phase can be conveniently described using the so-called conditional thermodynamic potentials $G(T,\ \boldsymbol{P},\ \boldsymbol{E})$ and $F(T,\ \boldsymbol{P},\ \boldsymbol{D})$ [14] which depend on the macroscopic polarization $\boldsymbol{P}$. Here the equilibrium polarization is determined by minimization of these potentials with respect to $\boldsymbol{P}$. Thus, the polarization at fixed $\boldsymbol{E}$ is determined by the following equation:

$$\left.\frac{\partial F(T,\boldsymbol{P},\boldsymbol{E})}{\partial \boldsymbol{P}}\right|_{T,\boldsymbol{E}} = 0 \tag{4}$$

while the polarization at fixed $\boldsymbol{D}$ is expressed as

$$\left.\frac{\partial G(T,\boldsymbol{P},\boldsymbol{D})}{\partial \boldsymbol{P}}\right|_{T,\boldsymbol{D}} = 0. \tag{5}$$

In the ferroelectric nematic phase the conventional thermodynamic potentials depend also on the nematic tensor order parameter $Q_{ij} = D(n_i n_j - \frac{1}{3}\delta_{ij})$, i.e., $F = F(T,\ Q_{ij},\ \boldsymbol{P},\boldsymbol{E})$ and $G = G(T,\ Q_{ij},\ \boldsymbol{P},\boldsymbol{D})$, where the nematic tensor order parameter is also determined by minimization of the corresponding potential.

It has been shown [16,17] using the molecular-statistical approach that the potential $G = G(T,\ Q_{ij},\ \boldsymbol{P},\boldsymbol{D})$ can be expressed in the following general form:

$$G(T,Q_{ij},\boldsymbol{P},\boldsymbol{D}) = \int d\boldsymbol{r} G_0(Q_{ij},\boldsymbol{P},T) + \frac{\epsilon_0}{2}\int d\boldsymbol{r}\boldsymbol{E}(\boldsymbol{r})^2, \tag{6}$$

where $\epsilon_0\boldsymbol{E}(\boldsymbol{r}) = \boldsymbol{D}(\boldsymbol{r}) - \boldsymbol{P}(\boldsymbol{r})$ is the actual electric field in the ferroelectric material, with $\boldsymbol{r}$ denoting position. The last term in Eq. (6) is the energy of the electrostatic field in the volume of the sample which can be expressed as the average of the sum of the interactions between all molecular dipoles, the interaction between molecular dipoles and the external electric field E_0 created by the external charges, and the electrostatic energy of the external field itself.

In a flat LC cell with homogeneous charge density on the electrodes, the electric field is normal to the surface for symmetry reasons, i.e., $\boldsymbol{E} = (0, 0, E_z)$, where the z axis is perpendicular to the cell surface. Hence $\epsilon_0 E_z = D_z - P_z$. One notes also that in such a cell, $D_z = \text{const} = \epsilon_0 E_0$ where E_0 is the electric field created by fixed charges on the electrodes. Thus, the potential density per unit area $G(T,\ Q_{ij},\ \boldsymbol{P}, D_z)$ can be expressed in terms of D_z in the following way:

$$G(T, Q_{ij}, \boldsymbol{P}, D_z) = \int dz G_0(Q_{ij}, \boldsymbol{P}, T) + \frac{1}{2\epsilon_0} P_z^2 - \frac{1}{\epsilon_0} D_z P_z + \frac{1}{2\epsilon_0} D_z^2. \tag{7}$$

The last three terms in Eq. (7) have a distinct physical meaning. The term $(\frac{1}{2\epsilon_0})P_z^2$ is the so-called self-energy, which is the average of the total dipole-dipole interaction, while the term $-D_z P_z/\epsilon_0$ is a coupling between molecular dipoles and the external field. Finally, the last term is the energy of the external field.

In Eq. (6), $G_0(Q_{ij},\ \boldsymbol{P},\ T)$ is the part of the thermodynamic potential density which is determined by short-range intermolecular interactions. Thus, according to the general Landau-de Gennes theory, it can be expanded in terms of the spontaneous polarization $\boldsymbol{P}(z)$ and the nematic order parameter Q_{ij}.

Taking into consideration the lowest order term in Q_{ij} and the gradient term in the polarization one obtains

$$G_0(Q_{ij}, \boldsymbol{P}, T) = \frac{1}{2}\alpha(T - T_c)P^2 - \frac{1}{2} B P_i Q_{ij} P_j + \frac{1}{4} b P^4 + \frac{1}{2} g\left(\frac{dP_i}{dz}\frac{dP_i}{dz}\right). \tag{8}$$

In Eq. (8), T_{c} is a critical temperature, α and b are Landau coefficients, B describes the coupling between polarization and the nematic tensor order parameter, and the term $\frac{1}{2}g(\frac{dP_i}{dz}\frac{dP_i}{dz})$ is the gradient term. Now the expression for the free energy $F = F(T,\ Q_{ij},\ \boldsymbol{P}, \boldsymbol{E})$ can be obtained using the Legendre transformation:

$$\frac{1}{\sigma}\int dz F(T, Q_{ij}, \boldsymbol{P}, E_z) = \frac{1}{\sigma}\int dz G(T, Q_{ij}, \boldsymbol{P}, D_z) - \int dz E_z D_z. \tag{9}$$

Here the last term can be expressed as

$$\int dz E_z D_z = d E_{av} D_z, \tag{10}$$

where $E_{av} = \frac{1}{d}\int dz E_z(z)$ is the average electric field and d is the cell thickness. Expressing also $D_z = \epsilon_0 E_{av} + P_{z,av}$, where $P_{z,av} = \frac{1}{d}\int dz P_z(z)$ is the average z component of the polarization, one obtains

$$\frac{1}{\sigma}\int dz F(T,\ Q_{ij},\ \boldsymbol{P}, E_z) = \int G_{\text{short}}(T,\ Q_{ij},\ \boldsymbol{P}(z))dz + \frac{1}{2\epsilon_0}\int \left[P_z^2(z) - P_{z,av}^2\right]dz - V P_{z,av} - \frac{\epsilon_0}{2}E_{av}^2, \tag{11}$$

where the applied voltage $V = E_{av} d$.

It is important to note that the free energy F contains the nontrivial self-energy term $\frac{1}{2\epsilon_0}\int[P_z^2(z) - P_{z,av}^2]dz$, which is nonzero only in the case of inhomogeneous polarization, in the ferroelectric phase. This term is usually ignored in the literature because of the wrong assumption that the general form of the free energy in the case of inhomogeneous polarization is the same as in the case of the homogeneous one. In the latter case the self-energy term vanishes and the free energy has the familiar form.

Now let us consider qualitatively the polarization switching in the N_f phase under the action of an oscillating applied voltage, as occurs in a typical experiment. It is reasonable to assume that in the case of very large polarization the modulus of polarization remains constant and the polarization vector just rotates locally or globally. In the general case, the polarization must overcome some potential barrier to reverse its direction. The type and height of this potential barrier can be determined from the free energy functional (11). In this functional the potential barrier may be determined by the gradient term $\frac{1}{2}g(\frac{dP_i}{dz}\frac{dP_i}{dz})$ and by the self-energy term which are important in the case of inhomogeneous polarization.

B. Anchoring energy and alignment

In considering the surface anchoring energy for ferroelectric nematic materials it should be noted that there are two contributions: first, the normal anchoring energy associated with any nematic (referred to here as the orientational anchoring energy), and a second contribution which is the polar anchoring energy, ω. In this section, we consider the latter, which is expected to be much larger than the orientational contribution in materials with large polarization. This can be seen through the following arguments. The simplest mathematical form of such a surface energy is $\frac{1}{2}\omega P_{z,s}^2$ where $P_{z,s}$ is the z component of the polarization at the surface and ω is the corresponding anchoring strength.

If the anchoring strength ω is relatively small, the polarization may rotate homogeneously overcoming the surface potential barrier. The height of this potential barrier can be estimated as ωP_0^2. Now, the experimentally determined polarization at a given applied voltage before saturation can be estimated roughly assuming that total energy of interaction with the average electric field, which can be estimated as PV, is of the same order as the height of the potential barrier:

$$\omega P^2 \sim PV. \tag{12}$$

Equation (12) can now be used to obtain a very crude estimate of the experimentally observed polarization $P \sim \omega^{-1} V$. This estimate is valid only if the polarization P appears to be less than the modulus of the equilibrium polarization P_0. At some value of the applied voltage V the polarization P reaches P_0, and this enables one to estimate the voltage $V \sim \omega P_0$, which corresponds to the saturation of the measured polarization. Thus, even in the situation where the polar anchoring energy is significant, we arrive at the same general conclusion that the saturated value of spontaneous polarization, P_0, is determined by the applied voltage, rather than the applied field. Physically, this is because the polarization during switching always has to overcome some potential barrier.

In the opposite case, the anchoring energy is sufficiently strong and the polarization cannot switch by overcoming the surface potential barrier. In this case it is more energetically favourable to form a diffuse domain wall which separates the regions with opposite polarization. The typical rate of change of the polarization in the boundary region as well as its thickness can be estimated as $r_w \sim [g/\alpha(T - T_c)]^{1/2}$. Then the height of the potential barrier during switching is determined by the polarization deformation energy in the boundary region:

$$\int \left(\frac{dP_i}{dz}\frac{dP_i}{dz}\right) dz \;\sim\; gP^2 r_w^{-1}. \tag{13}$$

Similar to the previous case, one may assume that the height of this barrier should be of the same order of magnitude as the total energy of interaction with the applied electric field, i.e., $gP^2 r_w^{-1} \;\sim\; PV$, and hence one obtains the following estimate for the experimentally measured polarization $P \;\sim\; \frac{1}{g} r_w V$. The applied voltage required to reach the saturation of the polarization is then estimated as $V \;\sim\; P_0 g r_w^{-1}$.

The relationship between the effects of an alignment layer and cell thickness can also be described mathematically. Let l be the thickness of the boundary dielectric layer (i.e., alignment layer) with dielectric constant ϵ, and L be the total thickness of the boundary layers plus the LC layer. Also let E_d be the electric field in the boundary layer and E_{lc} be the electric field in the N_f phase. Now we have two equations for these fields; the first equation follows from the fact that the displacement D_z is constant across the cell. One obtains

$$\epsilon_0 \epsilon E_d = \epsilon_0 E_{lc} + P_z, \tag{14}$$

where P_z is the z component of the polarization in the N_f phase.

The second equation is

$$(L - 2l)E_{lc} + 2lE_d = V, \tag{15}$$

where V is the applied voltage, i.e., the equation states that the sum of the potential differences across the alignment layer and the nematic layer is equal to the applied voltage.

Now let us look at the orders of magnitude. Typical polarization is 5 μC cm^{-2}, which is equivalent to the electric field $E_p = \epsilon_0^{-1} P \;\sim\; 5000\,\text{V}\mu\text{m}^{-1}$. Physically this is a field in the homogeneous homeotropic cell without alignment layers and with disconnected electrodes, filled with a typical ferroelectric nematic. Indeed, in this case $D_z = \epsilon_0 E + P_z = 0$ and hence $E = \epsilon_0^{-1} P_z$. This field is several orders of magnitude higher than the average applied field $E_0 = V/L$, which is of the order of 1 V μm^{-1}.

The simultaneous Eqs. (14) and (15) can be readily solved to express the fields E_d and E_{lc} analytically. Using the small parameters $l/E \ll 1$ and $\epsilon_0 E_0 / P_z \ll 1$, one obtains the following approximate expressions:

$$\begin{aligned} E_d &\approx \frac{1}{\epsilon_0 \epsilon} P_z, \\ E_{lc} &= E_0 - \left(\frac{l}{L}\right)\left(\frac{1}{\epsilon_0 \epsilon}\right) P_z \\ &= E_0 \left[1 - \frac{1}{\epsilon}\left(\frac{l}{L}\right)\left(\frac{P_z}{\epsilon_0 E_0}\right)\right]. \end{aligned} \tag{16}$$

From this, we can draw the following conclusions: firstly, the field E_d in the dielectric alignment layer is determined by the spontaneous polarization and is orders of magnitudes larger than the average applied electric field E_0 and the field in the N_f layer. Second, the field in the nematic layer E_{lc} is the difference of two terms, where the first term is the average field E_0 and the second term is proportional to polarization P_z and the small parameter l/L. Thus, the ratio of the second and first term is proportional to the product of the small parameter l/L and the large parameter $P_z/\epsilon_0 E_0$. As a result, the second term may be of the order of E_0 or even larger for sufficiently large polarization P_z or small cell thickness L.

The ratio l/L can be of the order of 10^{-3}–10^{-4} depending on the cell thickness L. Assuming that $\epsilon \sim 2.5$, one obtains the following estimate:

$$\left(\frac{l}{L}\right)\left(\frac{l}{\epsilon_0 \epsilon}\right) P_z \sim 0.2\text{–}2.0\,\text{V}\mu\text{m}^{-1}. \tag{17}$$

Thus, at relatively small L the second term may be larger than the first term E_0, and as a result the actual field in the N_f layer possesses the same sign regardless of the sign reversal of the field E_0 when the applied voltage is alternating. In thicker cells the second term may be smaller than the first one but of the same order. As a result, we predict that the switching behavior of N_f materials in cells with an alignment layer is highly thickness-dependent; in thinner cells, there may be no switching at all, while in thicker cells, the saturation voltage should be several times higher compared with cells without alignment layer because the actual field in the N_f layer, E_{lc}, is smaller than V/l.

The key predictions from this work are that (i) the polarization of N_f materials measured experimentally is a function of the applied voltage and not of the average electric field, and (ii) that the polarization switching in cells with and without alignment is very different. These predictions are explored experimentally in a later section.

C. Possible effects of charge accumulation

The nematic material used in this paper is characterized by a very low ionic content. However, in the general case ionic carriers can play a role, including in particular the dynamics of ferroelectric nematic LCs. Here we consider the equilibrium properties of the N_f phase, and in this case the electric field E_{lc} inside the nematic layer separates the ionic charges creating two double layers at the boundaries between the nematic layer and the alignment layers. The thickness of such a double layer is of the order of the Debye screening length ξ_D, and hence the ion carriers increase the effective thickness of the alignment layer l. This leads to an increase of the second term in Eq. (16), which reduces the electric field in the nematic layer. In addition, the ionic charges may partially screen the spontaneous polarization leading to its effective decrease. This effect, however, is less important in the case of very large polarization.

The dynamics of ferroelectric nematic LCs as well as the frequency-dependent dielectric constant may be strongly affected by charge carriers. In particular, the ion carriers are responsible for the $\epsilon_A^{'}(\omega)$ tail at low frequencies. The ionic current can also make a contribution to the polarization

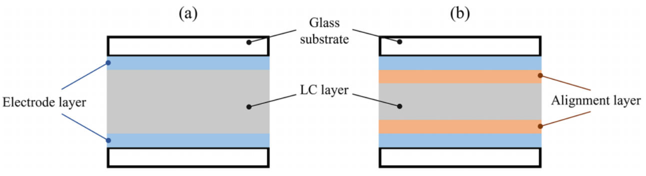

FIG. 2. Simplified schematics of sample cells. (a) Geometry of cells with no alignment layer, only an electrode layer. (b) Geometry of cells with both electrode and alignment layer included. The electrodes are indium-tin oxide and where an alignment layer is included in the cell, it is applied to the innermost surface of the electrodes, directly adjacent to the LC. The thicknesses of the electrode and alignment layer are very thin, such that there is a negligible difference to the thickness of the LC layer. Schematic not to scale.

current during the process of ferroelectric switching making the switching dynamics more complicated. These dynamic effects are beyond the scope of the equilibrium theory developed in this paper.

III. METHODS

A. Material

The LC mixture FNLC-919 is investigated here, provided by Merck Electronics KGaA. The phase sequence is as follows $\mathrm{Cr} \overset{8\,^{\circ}\mathrm{C}}{\leftrightarrow} N_f \overset{32\,^{\circ}\mathrm{C}}{\leftrightarrow} N_x \overset{44\,^{\circ}\mathrm{C}}{\leftrightarrow} N \overset{80\,^{\circ}\mathrm{C}}{\leftrightarrow} I$. Importantly, the mixture exhibits the N_f phase at room temperature, with a nonpolar nematic phase, N, and a second nematic phase, denoted here as N_x, at higher temperatures. The N_x phase has been shown to have some antiferroelectric character [7] and is also referred to as the smectic-Z phase [16] but is not discussed further here. All phases are enantiotropic.

B. Measurement of polarization

The measured polarization throughout the Experimental Results section of this paper is denoted as P_S, with the maximum value of P_S being equivalent to P_0 as in the Theoretical Discussion section. Samples were prepared by capillary filling the LC in standard sandwich-type glass cells, shown schematically in Fig. 2, with varying cell gap thicknesses of $d = 4\,\mu\text{m}$, $10\,\mu\text{m}$, $23\,\mu\text{m}$, and $46\,\mu\text{m}$. All cells have a coating of indium-tin oxide (ITO) to form the electrode layer on the inner glass substrates. Two different types of cells were used: cells with no alignment layer, so there is direct contact between the LC and ITO layer, and cells with a homeotropic (HT) alignment layer on the inner surface of the ITO, adjacent to the LC layer. All cells are purchased from INSTEC (Boulder, Colorado, USA) and the AWAT PPW Company (Warsaw, Poland), or provided by Merck Electronics KGaA (Darmstadt, Germany).

It is clear from the theoretical discussion above that the effective electric field in a device filled with N_f material is significant, a factor that could lead to the degradation of the LC itself. Therefore, the sample preparation conditions were varied, by (1) filling the sample cell in nonpolar (I, N) or polar (N_f) phases, and (2) changing whether the electrodes were (a) connected (no charge on the substrate) or (b) disconnected during filling. Measurements for samples with all combinations of these variables were repeated over the course of 5 wk, to probe the stability of the response, longevity of the sample, and the reproducibility of the measurements.

The spontaneous polarization was measured at room temperature using the current reversal technique [18] wherein a triangular waveform AC voltage is applied to a sample and the current flow resulting from reorientation of the N_f phase is recorded. Measurements of P_S were undertaken for a range of applied voltages at a frequency of 63 Hz, at room temperature. The accuracy of the measurements is dependent on the quality of the *Ps* curve, although it is small, with standard deviation in the P_S measurement of all samples after the saturation point being on average 0.01.

IV. RESULTS AND DISCUSSION

A. Effect of filling conditions on switching

We consider first the effect of filling conditions on the reproducibility of measurements of the spontaneous polarization of FNLC-919. Figures 3(a)–3(c) show the spontaneous polarization as a function of voltage for cells with no alignment layer filled with connected top and bottom electrodes, while for Figs. 3(d)–3(f) they are disconnected. Measurements are repeated over a 5 wk period.

It can be seen from Fig. 3 that the initial measured saturated P_s takes a value of $5.4 \pm 0.2\,\mu\text{C}\,\text{cm}^{-2}$ in all cases. There is effectively no difference seen in cells filled connected or disconnected. However, there are small but significant differences observed over the testing period of 5 wk that depend on the filling conditions, particularly the phase of the LC during filling, summarized in Fig. 4. When the cells are filled in the nonpolar (isotropic or nematic) phases, we observe small variations in the P_s that appear dependent on the cell thickness. We estimate the uncertainty in the P_s measurements to be $\pm 0.05\,\mu\text{C}\,\text{cm}^{-2}$ on the basis of repeated measurements.

The most apparent changes are observed in samples prepared in the N_f phase [Figs. 3(c) and 3(f)], where in cell gaps of $10\,\mu\text{m}$ there is a significant decrease from $P_S \sim 5.4\,\mu\text{C}\,\text{cm}^{-2}$ to as low as $4.8\,\mu\text{C}\,\text{cm}^{-2}$ over the course of 5 wk of testing. A decrease is also observed in the $23\,\mu\text{m}$ cell gaps, from values of $P_S \sim 5.3\,\mu\text{C}\,\text{cm}^{-2}$ to approx. $5.1\,\mu\text{C}\,\text{cm}^{-2}$. Interestingly, no such response degradation is seen in the $4\,\mu\text{m}$ and $50\,\mu\text{m}$ samples, indicating that some control can be exerted over the quality of the sample by varying the sample thickness. The thin samples retain the most consistent response across all preparation and testing conditions. The most significant change is seen in cells with LC layer thickness $d = 10\,\mu\text{m}$, prepared in the N_f phase. It is not unreasonable to conclude polar interactions at the surface boundaries are at the base of these changes.

For the remaining tests we will focus on cells filled in a nonpolar phase, as for them P_S in all cell gaps remains consistent over time.

B. Voltage dependence of P_S measurements

One of the key predictions of the theoretical section was that the P_s in a N_f material should saturate at a specific voltage rather than field. Figure 5(a) shows data for a variety of cell thicknesses with no alignment layer; it is clear that in thicker

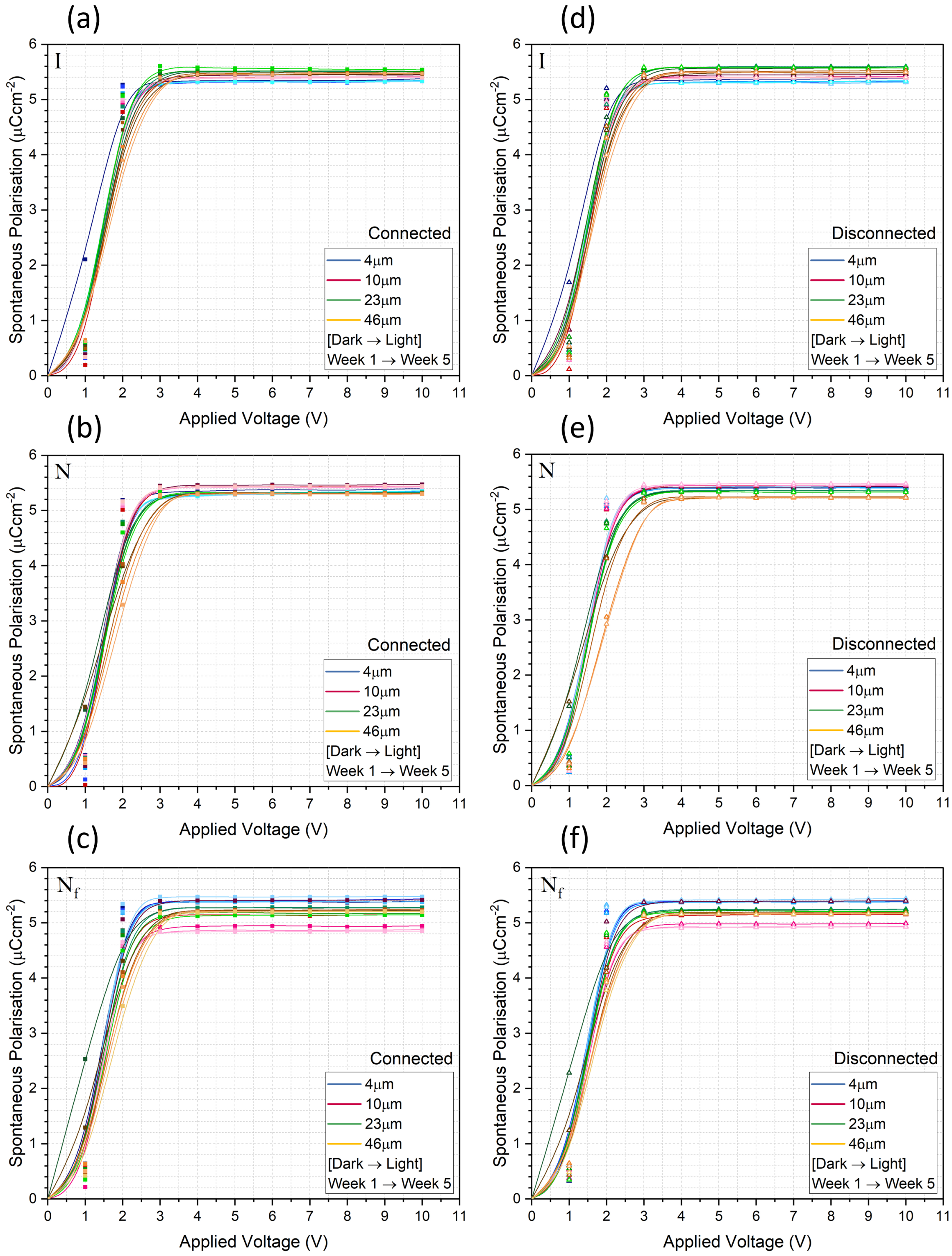

FIG. 3. Effect of filling conditions on P(V) tests. The first column (a)–(c) includes samples prepared with the electrodes in the connected state; the second column (d)–(f) includes those with electrodes in the disconnected state. Each row shows results for samples filled in one of three phases: (a) and (d) are filled in the isotropic phase, (b) and (e) are filled in the nematic phase, and (c) and (f) are filled in the ferroelectric nematic phase. The voltage is applied as V_{RMS}.

cells, the threshold field for saturation decreases. Figure 5(b) shows the same data as a function of applied voltage, where it is apparent that saturation is reached, in this case, at 3 V.

This is exactly as proposed in the theory section, i.e., there exists a potential energy barrier which must be overcome to achieve full switching. This suggests that we are indeed in a

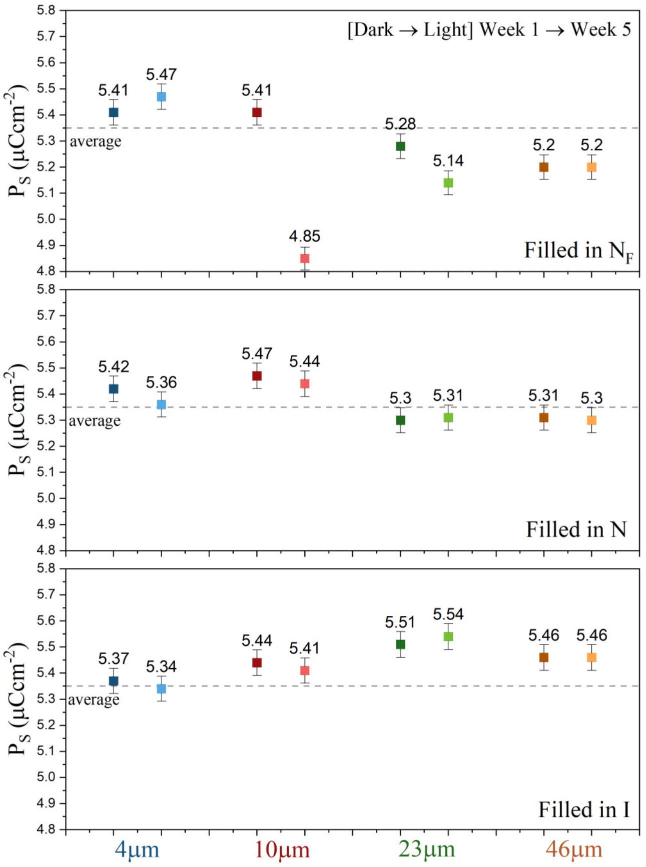

FIG. 4. Summary of saturated P_S values over the period of 5 wk in cells with varied preparation conditions, all in the connected state.

very weak anchoring regime when no alignment layer is used. We also observe a very small thickness dependence of the saturated value of P_s, with thinner cells giving a somewhat lower value than the thicker ones. We interpret this as a consequence of a very small, but nonzero orientational anchoring energy at the ITO substrate. We note, however, that the difference is close to the estimated uncertainty in the data.

C. Effect of alignment layer on switching

As discussed above, in addition to the case where the anchoring energy is small and effectively negligible, we expect the inclusion of an alignment layer in the cell to provide a barrier that is large enough that overcoming it becomes difficult or even impossible. To explore this, experimentally, we compare cells with no alignment layer (only an ITO electrode layer) with cells with a polyimide homeotropic alignment layer. One expects that polar anchoring energy will be significantly larger due to this inclusion of a dielectric layer because of strong electrostatic interactions with the ferroelectric layer. Results from the polarization tests for both cases are shown in Fig. 6.

We consider first details of the polarization switching in the cells with no alignment layer. In this case the polarization reaches saturation at 3 V and in both thin (10 μm) and thick (46 μm) cells, a single polarization peak is characteristic of the switching, as can be seen in Fig. 6. However, when the homeotropic polyimide alignment layer is present, we see a polarization response only in the thick (50 μm) cell. The polarization switching is clearly complex; the saturation voltage in the thick cell is ~9 V and the switching profile is not a single current peak as might be expected, but formed from multiple smaller peaks merging as the applied voltage is increased. The maximum polarization P_0 appears unaffected by the presence of the alignment layer.

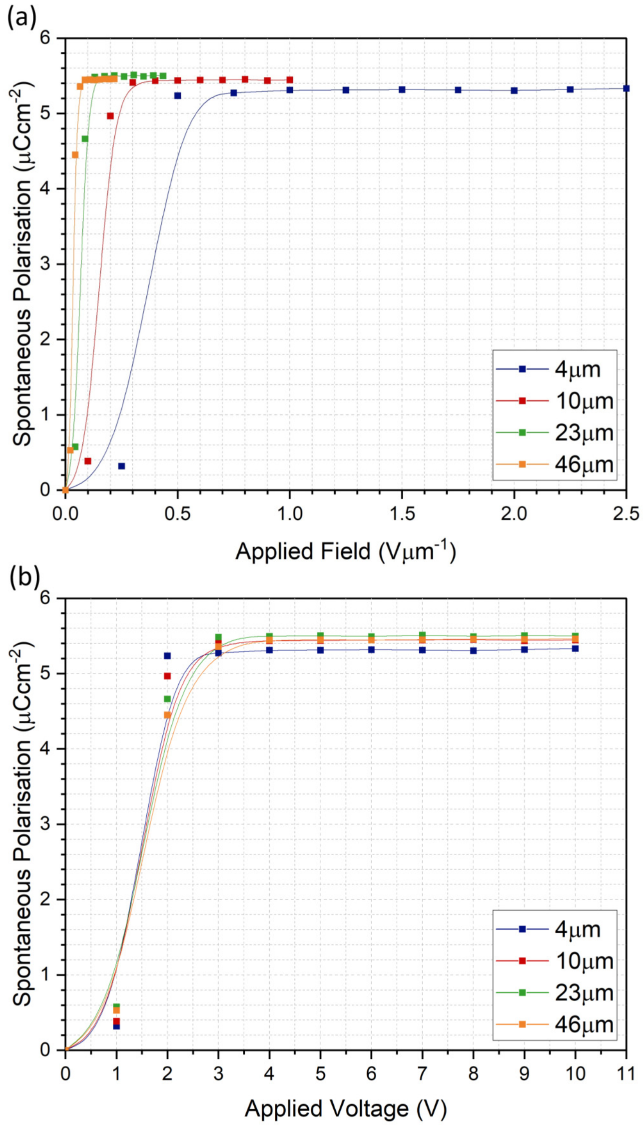

FIG. 5. Comparison of polarization tests in the four cell gap thicknesses plotted against (a) applied field and (b) applied voltage. The relationship $E = V/d$ is used to transform voltage into field.

The effects of thickness and alignment layer are perhaps most obvious when electrode gaps of ~1 mm (rather than microns) are used to measure the spontaneous polarization. Electroporation cuvettes with gaps of 1 mm and 4 mm were used for this purpose. [19] In such cuvettes, a voltage comparable to that needed in homeotropically aligned cells was sufficient to achieve saturation of the P_S response. Figure 7 shows the switching curves measured in these cuvettes with applied voltage of 320 V at 20 Hz. The electrodes in the cuvettes are aluminum and have no alignment layer, but have

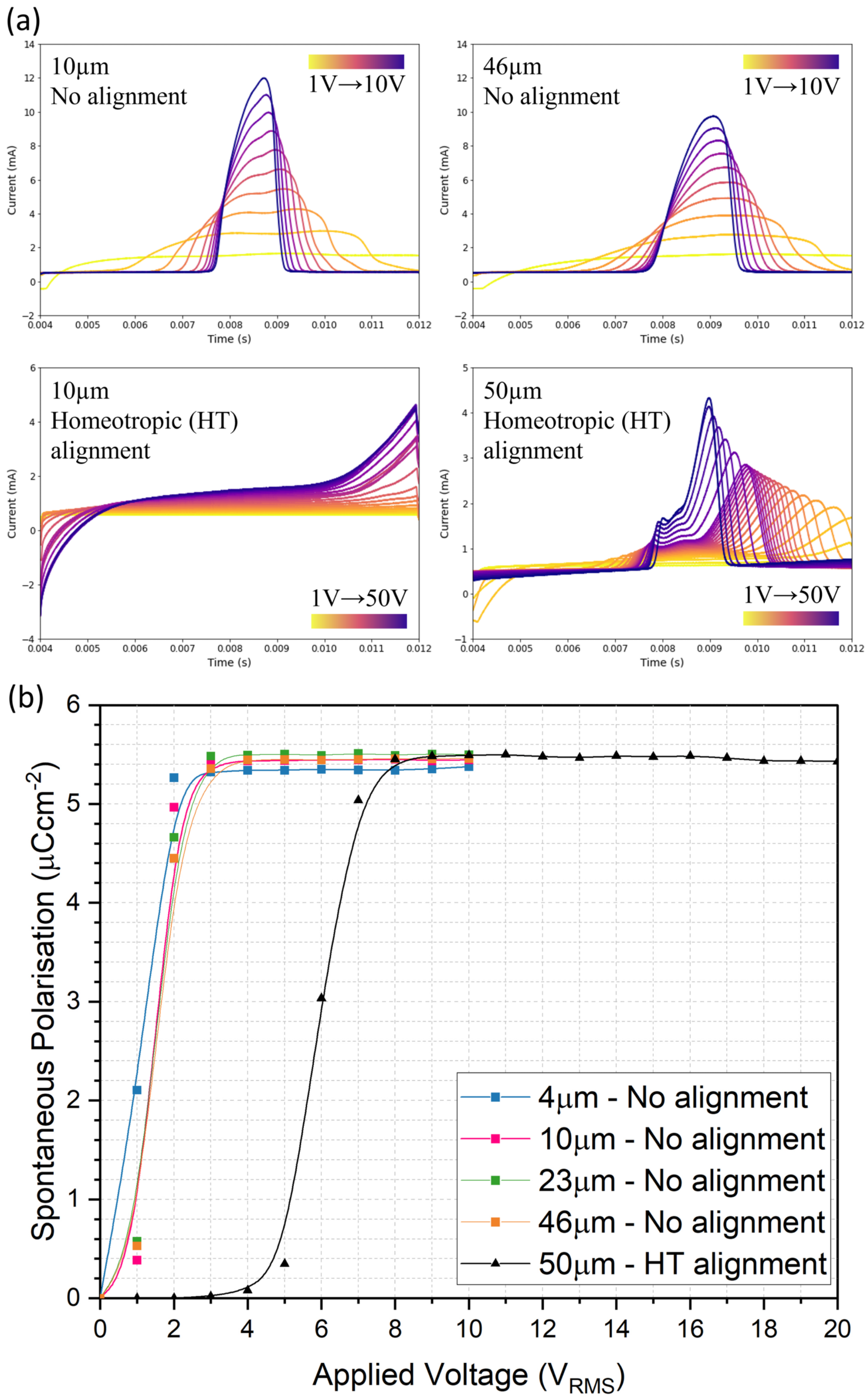

FIG. 6. (a) Current response traces in thin (∼10 µm) and thick (∼50 µm) cells, both unaligned and with a homeotropic (HT) alignment layer. (b) P(V) curves showcasing the difference in polarization response in unaligned cells vs one with homeotropic alignment. Note that the maximum voltage applied in the case of the homeotropically aligned cells is 50 V, rather than 10 V in the case of the unaligned cells.

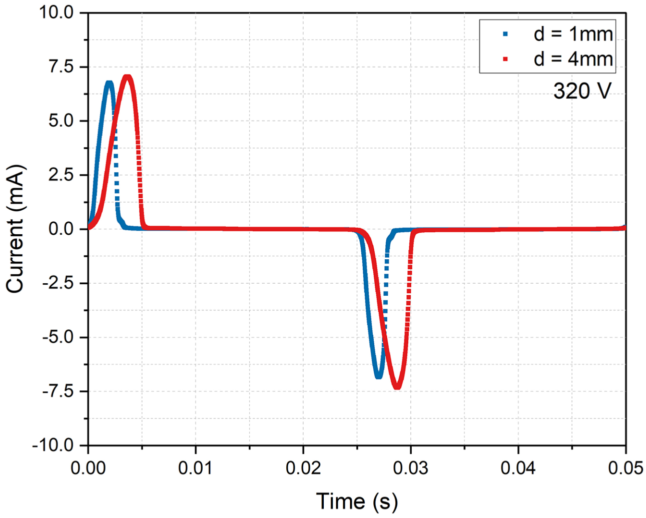

FIG. 7. Current responses obtained in cuvettes with electrode separations of 1 mm and 4 mm, with applied voltage of 320 V at 20 Hz.

an intrinsic, insulating aluminum-oxide surface. The switching curves are extremely uniform, with no hint of additional peaks and a very flat baseline. This is attributed to the cuvette geometry approaching the ideal for the polarization switching of the ferroelectric nematic fluid.

V. CONCLUSIONS

In this paper we have studied in detail the polarization switching in ferroelectric nematic LC cells. The derivation of the thermodynamic potential allowed us to make some specific predictions that we have tested experimentally. Perhaps the most important result is that it is the applied voltage rather than electric field that controls the polarization switching in N_f materials, such that there is a critical voltage at which the P_s reaches a saturated value, P_0. The theory presented indicates that this is because full polarization switching is achieved by the overcoming of a potential barrier which should be compared with the full energy of the coupling with the external field and not with the local energy density. The threshold voltage is observed experimentally. Indeed, the full energy is an integral of $(P\dot{c}E)$ over the layer thickness which is proportional to the applied voltage V.

We consider also the influence of surface anchoring energy on the potential barrier and thus the switching behavior. Two cases are described: a case where there is weak polar anchoring and strong polar anchoring. In the experimental procedure, we treat an unaligned LC cell with only a conducting ITO layer as the first case, and a cell with a dielectric (but nonconducting), homeotropic alignment layer as the second. The spontaneous polarization will naturally interact differently with conducting and nonconducting surfaces. In the aligned case, we observe an increase in the potential barrier represented as an increase in the threshold voltage to reach P_0. This is due to strong electrostatic interaction between the large molecular dipoles and their images in the conducting medium which promotes homeotropic anchoring.

One notes that the explanation provided of the voltage dependence of polarization assumes the corresponding potential barrier is independent of cell thickness and is determined by the anchoring strength. However, it has been shown that sample thickness makes a difference in the case of a thin cell with strong anchoring energy. The presence of the dielectric boundary layer means that the potential barrier may become insurmountable due to insufficient volume of the ferroelectric material; in other words, one may observe an apparent thickness-dependence because of the presence of this boundary layer. Further, in very thin cells with weak anchoring the dependence on thickness may be more complicated because of the dependence of the elasticity energy of the domain wall on thickness.

We observe also that surface polar interactions have an effect on the quality and longevity of a ferroelectric sample. Specifically, when prepared in a nonpolar phase, the polarization response of the LC remained stable over the testing period of 5 wk; on the other hand, when prepared in the ferroelectric phase, we see a degradation in the saturated polarization P_0. This effect is stronger in some cell thicknesses than others. There are no significant differences in cells prepared while in a connected or disconnected state. These findings have implications not only to the study of the ferroelectric nematic LC phase, but to the treatment of strongly polar fluids in general.

ACKNOWLEDGMENTS

H.F.G. acknowledges funding from the EPSRC, Grant No. EP/V054724/1. D.N. and H.F.G. acknowledge Merck Performance Materials Ltd. for funding and the provision of materials.

DATA AVAILABILITY

The data that support the findings of this article are openly available [20].

---

[1] A. K. Bain and P. Chand, *Ferroelectrics: Principles and Applications* (Wiley-VCH Weinheim, 2017).

[2] *Handbook of Liquid Crystals*, edited by J. W. Goodby, P. J. Collings, T. Kato, C. Tschierske, H. F. Gleeson, and P. Raynes (Wiley-VCH Weinheim, 2014).

[3] R. J. Mandle, S. J. Cowling, and J. W. Goodby, A nematic to nematic transformation exhibited by a rod-like liquid crystal, Phys. Chem. Chem. Phys. **19**, 11429 (2017).

[4] H. Nishikawa, K. Shiroshita, H. Higuchi, Y. Okumura, Y. Haseba, S. Yamamoto, K. Sago, and H. Kukichi, A fluid liquid-crystal materal with highly polar order, Adv. Mater. **29**, 1702354 (2017).

[5] M. Born, Üeber anisotrope Flüssigkeiten: Versuch einer Theorie der flüssigen Kristalle und des elektrischen Kerr-Effekts in Flüssigkeiten, Sitzungsber. Preuss. Akad. Wiss. **30**, 614 (1916).

[6] R. J. Mandle, S. J. Cowling, and J. W. Goodby, Rational design of rod-like liquid crystals exhibiting two nematic phases, Chemistry **23**, 14554 (2017).

[7] N. Sebastián, M. Čopič, and A. Mertelj, Ferroelectric nematic liquid-crystalline phases, Phys. Rev. E **106**, 021001 (2022).

[8] R. J. Mandle, A new order of liquids: Polar order in nematic liquid crystals, Soft Matter **18**, 5014 (2022).

[9] N. Sebastián, R. J. Mandle, A. Petelin, A. Eremin, and A. Mertelj, Electrooptics of mm-scale polar domains in the ferroelectric nematic phase, Liq. Cryst. **48**, 2055 (2021).

[10] H. Nishikawa, K. Sano, and F. Araoka, Anisotropic fluid with phototunable dielectric permittivity, Nat. Commun. **13**, 1142 (2022).

[11] A. Mertelj, L. Cmok, N. Sebastián, R. J. Mandle, R. R. Parker, A. C. Whitwood, J. W. Goodby, and M. Čopič, Splay nematic phase, Phys. Rev. X **8**, 041025 (2018).

[12] J. Li, H. Nishikawa, J. Kougo, J. Zhou, S. Dai, W. Tang, X. Zhao, Y. Hisai, M. Huang, and S. Aya, Development of ferroelectric nematic fluids with giant-ε dielectricity and nonlinear optical properties, Sci. Adv. **7**, 5047 (2021).

[13] O. D. Lavrentovich, Ferroelectric nematic liquid crystal, a century in waiting, Proc. Natl. Acad. Sci. USA **117**, 14629 (2020).

[14] L. D. Landau and E. M. Lifshitz, in *Electrodynamics of Continuous Media*, 2nd ed., edited by E. M. Lifshitz and L. P. Pitaevskii, Course of Theoretical Physics Vol. 8 (Elsevier, Moscow, 1984).

[15] M. A. Osipov, Dipole-dipole interactions and the origin of ferroelectric ordering in polar nematics, Liq. Cryst. 51, 2349 (2024).

[16] X. Chen, V. Martinez, E. Korblova, G. Freychet, M. Zhernenkov, M. A. Glaser, C. Wang, C. Zhu, L. Radzihovsky, J. E. Maclennan, D. M. Walba, and N. A. Clark, The smectic ZA phase: Antiferroelectric smectic order as a prelude to the ferroelectric nematic, Proc. Natl. Acad. Sci. USA **120**(8), e2217150120 (2023).

[17] K. Miyasato, S. Abe, H. Takezoe, A. Fukuda, and E. Kuze, Direct method with triangular waves for measuring spontaneous polarization in ferroelectric liquid crystals, Jpn. J. Appl. Phys. Part 2: Lett. **22**, L661 (1983).

[18] M. A. Osipov, On the origin of the ferroelectric ordering in nematic liquid crystals and the electrostatic properties of ferroelectric nematic materials, Liquid Crystal Rev. **12**, 14 (2024).

[19] Sigma-Aldrich, Darmstadt, Germany, https://www.sigmaaldrich.com/GB/en/product/sigma/z706078.

[20] https://doi.org/10.5518/1641.